Articles

Chinese Science Bulletin

Atmospheric Science

March 2010 Vol.55 No.7: 635–649
doi: 10.1007/s11434-009-0481-z

A new-generation sand and dust storm forecasting system GRAPES_CUACE/Dust: Model development, verification and numerical simulation

WANG Hong[1,2*], GONG ShanLing[1], ZHANG HongLiang[2], CHEN Yong[2,3], SHEN XueShun[2], CHEN DeHui[2], XUE JiShan[2], SHEN YuanFang[1], WU XiangJun[2] & JIN ZhiYan[2]

[1] *Centre for Atmosphere Watch and Services, Chinese Academy of Meteorological Sciences, Beijing 100081, China;*
[2] *State Key Laboratory of Severe Weather, Chinese Academy of Meteorological Sciences, Beijing 100081, China;*
[3] *State Key Laboratory of Numerical Modeling for Atmospheric Sciences and Geophysical Fluid Dynamics (LASG), Institute of Atmospheric Physics, Chinese Academy of Sciences, Beijing 100029, China*

Received February 20, 2009; accepted June 22, 2009; published online November 3, 2009

Based on the new-generation Global/Regional Assimilation and PrEdiction System (GRAPES) developed by the Numerical Prediction Research Center, China Meteorological Administration and the Chinese Unified Atmospheric Chemistry Environment for Dust Atmospheric Chemistry Module (CUACE/Dust) developed by the Centre for Atmosphere Watch and Services (CAWAS) of the Chinese Academy of Meteorological Sciences (CAMS), the China sand and dust storm forecasting system GRAPES /CUACE-Dust model has been established. The latest data of land desertification, optical properties of China sand and dust aerosols, daily soil moisture and snow cover over China main land was introduced in this system. The system showed good performance in mass conservation. The comparisons of real-time prediction outputs with surface observations and aerosol indices derived from TOMS ozone spectrophotometers (TOMS AI) indicate that the model can predict the outbreak, development, transport and depletion processes of sand and dust storms accurately over China and the East Asian region. The system makes real-time quantitative prediction of a series of elements including sand and dust injection from the surface, dry and wet deposition amount, dust concentration and optical depth. We selected 7 major dust storms occurring in April 2006 and analyzed the spatiotemporal distribution patterns of dust emission, dry and wet deposition and atmospheric load in this paper. The results showed that about 225 million tons of dust were emitted into the atmosphere from the deserts over east Asia in that month. The 3 major sand and dust sources were just as the following: The deserts in northern Inner Mongolia and the boundary area around China-Mongolia were the first dust sources with a contribution of 153 million tons accounting for 68% of the total emission. The Taklimakan Desert ranked second and contributed approximately 40 million tons accounting for 17% of the dust emission.The Onqin Daga Sandland emitted about 15 million tons or 7% of the total emission. The contributions from other deserts, sandy lands and abandoned farmlands were about only 8% of the total dust emission. The total deposition over the East Asian region in April 2006 was 136 million tons. The regional distribution of dust deposition showed that the 3 major sources were also the major deposition areas. The deposition amount in the 3 major sources accounted for 78% of the total with about 135 million tons falling back to the source regions. The secondary deposition area was the China mainland downriver, where more than 2 million tons deposited accounting for 16% of the total deposition. The deposition over the region east of 120°E including China off-shore regions, Korean Peninsula, Japan and the West Pacific took only 6% of the total deposition, which was about 850000 tons. The analysis on dry and wet deposition showed that dry deposition dominated in the process, accounting for 94% of the total sand and dust depositions in the period and wet deposition only was around for 6%, since it was generally dry with less rainfall over northern China in April.

mesoscale, sand and dust storm forecasting system, aerosol, dry deposition, wet deposition

Citation: Wang H, Gong S L, Zhang H L, et al. A new-generation sand and dust storm forecasting system GRAPES_CUACE/Dust: Model development, verification and numerical simulation. Chinese Sci Bull, 2010, 55: 635–649, doi: 10.1007/s11434-009-0481-z

*Corresponding author (email: wangh@cma.gov.cn)

In the arid and semiarid areas on the Earth, a large quantity of sand and dust aerosols was injected into the atmosphere under certain specific weather backgrounds annually. The particles suspended in the atmosphere driven by sand and dust storms have significant impacts on atmospheric environment [1], transportation, marine ecology (e.g. deposition in the ocean) [2], and acid rain nucleation [3]. Moreover, sand and dust particles also change the radiation balance of the earth-atmosphere system through absorbing and scattering solar and atmospheric long-wave radiations, and this can remodel the atmospheric temperature fields by heating or cooling it eventually leading to significant impacts on short-term weather systems and long-term climate change [4–11]. Accurate forecasts of the occurrence and development processes of such sand and dust storms not only meet the demands in severe weather forecasts, but also provide a basis for assessing direct and indirect effects of the dust aerosols on weather and climate.

The numerical models, including physical processes such as sand and dust emission, transport and deposition, play an important role in both research and operational forecast of sand and dust storm weather processes. Global atmosphere cycling models and regional climate models have unique advantages in describing the cycle of sand and dust particles in the atmosphere and their regional or global climatic effects [12–16]. However, due to the constraints of the global models in terms of temporal and spatial resolutions, as well as in describing detailed physical processes, their capability in predicting local sand and dust storms is limited. So far as the forecasting of sandy and dust storms occurring in certain areas is concerned, the mesoscale model has unparalleled advantages over global models in capturing the evolution of weather systems, refined temporal and spatial-resolution predictions, and in real-time data applications. From the late 1980s, some scientists began to use the mesoscale Numerical Weather Prediction (NWP) models to study and predict sand and dust weather over Sahara and Australia [17–19], while research on sand and dust storms in the East Asian region is relatively late [20–26]. However, recent results show that the East Asian dust uptakes from the deserts, Gobi and desertification farmland in western and northern China in conjunction with the areas around the China-Mongolian border make the most important contribution to the global dust emission. An estimated annual sand/dust emission from this region is about 800 million tons [27], sharing a substantial component in comparison with the global annual dust emissions 1–3 billion [10] or 1–5 billion tons [8]. The contribution of the East Asian dust to the global atmospheric sand and dust load is evidently greater than that from the Sahara Desert, in particular with a significant contribution to the dust load across the mid-latitudes (25°–40°N) in the Northern Hemisphere. Its impacts on the down-stream neighbors including the Korean Peninsula, Japan, the North Pacific, and even to west coast of the United States become a focus of extensive attention [20,21,25]. At the turn of the century, this region has experienced many long-distance sand/dust transport events, which has drawn increasing attention of the societies and earth science community. Currently, relative to other desert sources, it is a matter of urgency to enhance and to improve model-based research on sand and dust storm targeted to the East Asian region. For lack of observation data, the results on Sahara and Australian deserts were directly used in early model study and simulation of East Asian sand and dust events, varying from treatment of surface conditions, friction velocity and up-blowing sand and dust parameterization scheme to some optical properties and radiation parameters. However, compared with other dust sources, the East Asian dust sources are found diversity and complexity in surface conditions, land types: desert, Gobi Desert and waste farmlands due to desertification, as well as soil texture. Moreover, the season when sand/dust storm occurs and corresponding weather systems differ from those in other regions in the world. In general, any direct use of the observations and parameterization schemes developed for other deserts will inevitably lead to some uncertainties in model outputs. In recent years, as large-scale observations over the East Asian deserts, particularly in China deserts were carried out, a wealth of observation data were accumulated [1,26]. The question as to how to incorporate these latest observations into numerical models, to improve their performances and to predict the sand/dust event over the East Asian more accurately, is a very meaningful topic to address in current model-based research on the East Asian sand/dust.

Based on GRAPES-Meso model and a dust aerosol model focusing on the East Asian region (CUACE/Dust), a mesoscale sand and dust weather prediction system is established for both forecast and research of sand/dust storm events over East Asia in this paper. The most updated data including land surface, desertification, soil texture and the optical properties of sand and dust aerosols observed in this century in China are incorporated into the system, to make it more specifically relevant to sand and dust events in East Asia. This system can predict the sand/dust aerosol concentration, optical depth, uptakes and depositions on real-time.

1 Model description

The framework core of the GRAPES-CUACE/Dust model consists of two components, the mesoscale NWP model and the aerosol model. The GRAPES_Meso is adopted as the NWP model to drive the aerosol model [28–30], which is an integrated regional and global forecast system developed by NPRC/CMA with independent intellectual property. The CUACE/Dust model was developed by CAWAS/CAMS. The two models are coupled into GRAPES-CUACE/Dust and the transport and vertical diffusion schemes of dust aerosol were improved in light with the dynamical core and physical processes of GRAPES-Meso. The following 2 subsections briefly discuss the relevant works.

1.1 Mesoscale regional meteorological model−GRAPES-Meso

The GRAPES adopts a unified multiscale dynamic core, in which the horizontal resolution is adjustable, and the hydrostatic or nonhydrostatic approximation of the vertical motions is optional. The GRAPES-Meso consists of a 3-D data assimilation system, a dynamic framework, an optimized and improved parameterization scheme for physical processes [29,30]. GRAPES-Meso is designed to meet the requirements for mesoscale weather predictions, with its horizontal resolution being set at a higher level, while the vertical resolution adopts a nonhydrostatic approximation scheme. The model's temporal discretization adopts a semi-implicit & semi-Lagrangian temporal advection scheme [30]. The model grid is defined according to latitudinal and longitudinal points, and the horizontal spatial discretization is distributed with the Arakawa-C point variables and the second-order accuracy is maintained with a centered differentiation form [31]. To overcome Lagrangian trajectory errors under spherical coordinates at high latitudes, the vertical coordinates use a terrain tracking one, which gives more natural altitudes information. The vertical discretization adopts Charney-Phillips vertical isolate-layer variable setups to improve the calculation accuracy of vertical pressure gradient forcing [32]. A brief account is given below on the GRAPES dynamic framework and physical processes that are directly related to the sand and dust aerosol forecasts.

The transport terms (both horizontally and vertically) of sand and dust aerosols in GRAPES-CUACE/Dust model are calculated by the GRAPES-Meso dynamic framework. A QMSL semi-implicit & semi-Lagrangian scheme is adopted on each grid point in the model [30] and the total dust mass remains in conservation throughout the model integrating. The stability of Semi-Lagrangian and the mass conservation of trajectory tracking calculations schemes show a unique advantage in calculating the sand and dust transport term. In the process of model integration, the sand and dust concentration at $n+1$ time step on each grid point is derived from the following trajectory difference:

$$C_i^{n+1} = C_{i*}^{n} + \Delta t[(S+D)_i^{n+1}\alpha + (S+D)_{i*}^{n}\alpha], \qquad (1)$$

where C represents mass concentration of sand and dust aerosols. $n+1$ and n denote the $n+1$ and n time steps. i represents the size i within the 12 sand and dust particle size bin. S and D show the sand and dust source and sink terms respectively. Term with $*$ is the upstream point, a represents a weighted coefficient between the upstream point and the calculation point. Δt is the time of one step.

Based on an extensive investigation of the physical processes schemes for mesoscale forecasting model, targeted to the China and East Asian region, taking into full consideration of the weather and climate in China characterized with East Asian monsoon, and through a number of numerical experiments and comparative analyses, the authors of this paper have optimized the selected physical-process parameterization scheme of the GRAPES-CUACE/Dust model to make a reasonable sand and dust storm forecast. The physical processes of the present model include cumulus convection, microphysics, boundary layer, radiation, land surface, etc. The cloud precipitation scheme adopts the one that has been improved by CAMS/CMA modelers including an ice phase process. Numerical experiment results show that the precipitation intensity in the Chinese mainland based on this scheme is much more close to observations. The radiation scheme uses that of ECWMF, which captures reasonably well the detailed interactions between the surface radiation field and the topography, the 500-hPa pattern and the precipitation field over the Qinghai-Tibet Plateau. The boundary layer scheme has a direct impact on vertical diffusion of sand and dust aerosols, thereby affecting the transport and temporal & spatial sand and dust distributions. Numerical experiments show that the MRF boundary layer scheme [33] is superior to others in terms of calculating the vertical diffusion of sand and dust particles. The formula to calculate the vertical diffusion term is as the following:

$$\frac{\partial C_i}{\partial t} = \frac{\partial}{\partial z}\left[K_h\left(\frac{\partial C}{\partial z} - \gamma_c\right)\right], \qquad (2)$$

where C_i stands for dust/aerosol concentration, t for time, z for altitude, K_h for the heat vortex diffusion coefficient calculated by the MRF boundary layer scheme, γ_c for the contribution by local turbulence to the large-scale eddy current diffusion flux in GRAPES-Meso. For detailed discussion on the dynamic framework of the model, including its horizontal and vertical transport, the physical processes, e.g. boundary layer diffusion and the model performance, please refer to the Technical Report on New Generation General Multiscale Numerical Prediction System Operated in CMA [34].

1.2 Dust aerosol model CUACE/Dust

The dust aerosol model referred to in this paper was established by CAWAS/CAMS [35]. The model that includes such detailed processes as aerosol source, transport, dry and wet depositions, dust removal both in and below clouds, gives an explicit description about the interaction between aerosol and cloud. The aerosol mass balance equation is expressed as [34]

$$\begin{aligned}\frac{\partial \chi_{ip}}{\partial t} = {} & \frac{\partial \chi_{ip}}{\partial t}\Big|_{\text{Transport}} + \frac{\partial \chi_{ip}}{\partial t}\Big|_{\text{Sources}} \\ & + \frac{\partial \chi_{ip}}{\partial t}\Big|_{\text{Clear-air}} + \frac{\partial \chi_{ip}}{\partial t}\Big|_{\text{Day}} \\ & + \frac{\partial \chi_{ip}}{\partial t}\Big|_{\text{In-cloud}} + \frac{\partial \chi_{ip}}{\partial t}\Big|_{\text{Below-cloud}}.\end{aligned} \qquad (3)$$

The first term on the right stands for aerosol transport including the large-scale transport, sub-grid turbulence diffu-

sion and convection terms and it is calculated in the dynamic framework of the system. The second term represents aerosol source, including natural sources and man-made source emission process on the one hand, and taking into account secondary aerosol formation process on the other hand. The third term represents a clear-air process, including nucleation, condensation and aggregation. The fourth term describes dry deposition process, including the gases and aerosol particles. The fifth term defines an in-cloud removal process, including the cloud droplet activation, the interaction between aerosols, clouds and rain droplets and the cloud chemistry. The last term gives a below-cloud removal process, indicating the precipitation removal between a cloud layer and the surface. In the current dust aerosol forecasting system, the activated aerosol processes include the dust emission, transport, condensation, aggregation, dry deposition and below-cloud removal.

Based on observations of particle-size distribution over China desert, the model classifies sand/dust aerosol particles into 12 size bines, with particle diameter being 0.01–0.02 μm, 0.02–0.04 μm, 0.04–0.08 μm, 0.08–0.16 μm, 0.16–0.32 μm, 0.32–0.64 μm, 0.64–1.28 μm, 1.28–2.56 μm, 2.56–5.12 μm, 5.12–10.24 μm, 10.24–20.48 μm and 20.48–40.96 μm respectively. This dust model has been coupled with mesoscale meteorological model MM5 developed by NCAR and gave a reasonable simulation on dust events occurring in Northeast Asia [36].

To calculate radiation parameters in real time, e.g. sand/dust aerosol optical depth and to further calculate dust radiation effects, the authors have incorporated, on the basis of the above work, a detailed aerosol radiation parameterization module into the GRAPES-CUACE/ Dust model. The most fundamental factor for the radiation parameterization is the refraction index, which has a direct impact on the calculation of parameters like optical depth. The latest findings show that the refraction index of sand and dust aerosol in China significantly differs from that on Sahara and other deserts. Therefore, this paper introduces the latest desert sand and dust complex refraction indices [6] (see Figure 1) to calculate radiation parameters, e.g. optical depth. The main idea for this scheme is as the following: Firstly, taking into account the size bin of sand and dust particles at various scales in the GRAPES-CUACE/Dust model, the major optical properties of sand and dust aerosols are calculated with the refraction index according to the MIE scattering theory, including the extinction efficiency, single-scattering albedo and asymmetric factor depending on wavelength and particle radius. Secondly, the dust mass extinction coefficient and optical depth on each model grid are calculated from the extinction efficiency and the particle concentration outputted by the model. Finally, the dust optical depth, single-scattering albedo and asymmetric factor depending on wavelength on each model grid are obtained by weighted mean calculation of all dust size bins.

1.3 Model input parameters

Main ground parameters that affect dust emitting and dry deposition processes include such physical parameters as surface wind speed, land cover, soil particle size, soil moisture and snow cover and land cover status is one of the most fundamental factors determining the accuracy of dust emission. The present model takes into account 15 categories of the land cover. Their surface roughness is calculated with 1 km×1 km surface land use data of the BiosphereAtmosphere Transfer Scheme (BATS) [37]. However, for the regions in China, an updated desert map of China reflecting desertification processes from the 1980s to the early 21st century is used. The sand and dust up-blowing process is so sensitive to soil moisture that even a subtle change in it may cause a significant difference in the sand and dust uptake fluxes in the model. The sand and dust up-blowing scheme in the aerosol model requires the 0 –10 cm volume soil moisture (w_v). A number of numerical simulations and analyses show that the 0–10 cm mass moisture (w_g) in NCEP 1°× 1° reanalysis data proves effective in providing a sustained and stable model prediction. The w_v conversed by is w_g:

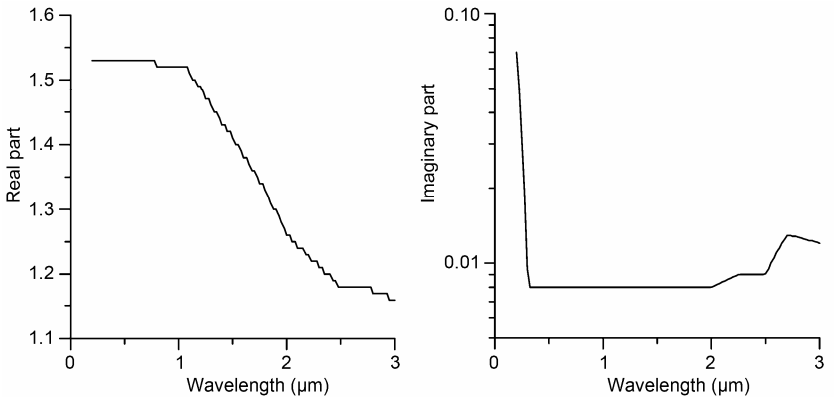

Figure 1 Dust aerosol complex refraction index in China desert.

$$w_g = \frac{w_v}{\rho_s}, \quad (4)$$

where ρ is a soil density derived through weighted averaging soil types at each grid point. At present, soil moisture data are input when the model integration starts and remains constant in the process of model integration. Theoretically, the changing of soil moisture can be triggered by precipitation and other factors in the model running process, which might lead to some errors in the dust predictions. However, the main dust sources in China or East Asia are mostly the deserts in mid-latitudes at an altitude exceeding 1500 m a.s.l., where the annual precipitation is very low and the sand and dust weather mostly occurs in the drier spring time. Moreover, GRAPES-CUACE/Dust model produces a forecast with normal time validity of 72 hours, during which such errors without considering the soil moisture changing would make little difference. When spring comes, the winter snow cover in the mid-latitudes over China begins to melt and a timely input of snow cover data is essential to an improved accuracy of the model prediction. In this paper, the NOAA 1°×1° satellite remote sensing data of snow cover is introduced in the model. The NCEP 1°×1° reanalysis data is used as the initial meteorological field and 6-hour lateral boundary conditions in the model.

2 Model verifications and the simulation results

The GRAPES-CUACE/Dust adopted identical grid distance. Its horizontal resolution is 0.25°×0.25° with 31 vertical layers from the Earth's surface to 30 km in the upper atmosphere. Its domain covers 70°–140°E and 15°–60°N, including the source regions of sand and dust storms in East Asia: southern Mongolia, China and down-stream areas: Korea, Japan, parts of the Western Pacific affected by the dust storms. From 1 March to 31 May 2006, GRAPES-CUACE/Dust model began its trial running. The model was run twice a day, with the initial time at 00 and 12 GMT respectively and with a prediction validity of 72 hours. This paper adopts the real-time model outputs at 00 hour from 1 to 30 April, during that period sand and dust storms are most frequent. The mass conservation in the model was verified first. Then, the sand and dust concentration and optical depth from the model for 72-hour predictions were compared with surface observations and TOMS aerosol index (TOMS AI), with a view to verifying the model's performance. Based on this, analysis was made on both spatiotemporal distributions and characteristics of the sand and dust emission, transport and deposition processes for the 7 main sand and dust storms in April 2006.

2.1 Model verification

As mentioned above, GRAPES-CUACE/Dust model uses a semi-implicit, semi-Lagrangian sand and dust transport scheme. The advantage of the positive shape-preserving advection scheme is to well keep the mass conservation of dust in the integrating process. According to the mass conservation calculation law, the inflows from the lateral boundary and the sand and dust uptakes in the model domain should be equivalent to the total outflows from the model's boundary, accumulated depositions and total suspending sand and dust particles in the atmosphere. As the model only considers the sand and dust sources in its domain, no sand and dust inflow is considered at the model's boundary. Therefore, the paper calculates the total accumulated sand and dust emission (in tons), dry and wet depositions (in tons), suspending sand and dust in atmosphere (in tons) and accumulative sand and dust outflows from the model's boundary (in tons) in the 72-hour integration for 30 days in April 2006. The comparison between the inputs and outflows (Figure 2) showed that the difference between the two was within 5% in the 72-hour integral process. Considering the errors in calculation of the total dust mass caused by volume calculation, the result suggested that the model has a good mass conservation in its integral processes.

2.2 Dust aerosol optical depth and surface sand and dust concentration

Observations [38,39] showed that there were 3 typical severe sand and dust storms (SDS) occurred over East Asia in April 2006, i.e. in 5–7 (SDS1), 9–12 (SDS2), 16–18 (SDS3) April respectively, while other 4 sand and dust storms (SD) took place on 8 (SD1), 21–23 (SD2), 24–25 (SD3) and 28–30 (SD4) April respectively. These sand and dust storms had an important impact on China and even on the East Asia

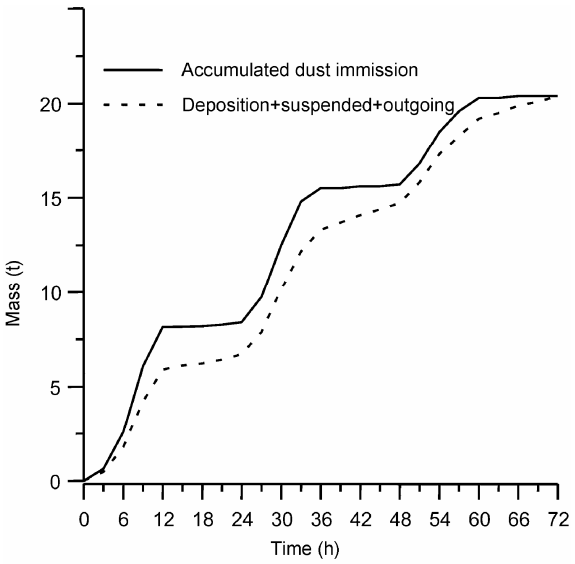

Figure 2 The accumulated dust emmission and the sum of total depositions, floating sand and boundary outflows.

as a whole. This paper intends to verify and analyze the model outputs of the 7 sand and dust events.

The dust aerosol optical depth (AOD) represents the extinction effect of sand and dust particles in the atmosphere from the earth's surface to the top level of the atmosphere. To verify the overall model performance in capturing the total sand and dust volume during each sand and dust event, the authors of this paper make the respective averaged AOD calculations in function to the wavelength during the 7 sand and dust events. Theoretically, the optical depth at the 0.55 μm wavelength generally represents the extinction due to the aerosols in the entire shortwave spectrum, therefore the authors select AOD at 0.55 μm wavelength to compare with the TOMS AI aerosol indices (see Figure 3). It should be noted the differences between dust AOD and TOMS AI when we compare the two. One is that AOD given by the model represents the total atmospheric extinction as result of sand and dust aerosols in the atmosphere (0–30 km) while TOMS AI has certain limitations in detecting atmospheric aerosols from the 2 km above the ground and the other is that TOMS AI is more sensitive to absorptive aerosols [40] but the sand and dust aerosols have relatively stronger scattering effect, especially those from the East Asian deserts, than that in other deserts. However, considering the fact that sand and dust aerosol could account for 70% of the total atmospheric aerosols over a desert and its adjacent down-stream areas when a sand and dust storm breaks out, TOMS AI still reflects, to a large extent, the overall extinction effects of dust aerosol in the atmosphere. The closer to the source, the more representative it will be. Thus, the sand and dust AOD given by the model has a good comparability with TOMS AI in East Asia.

The comparative analysis of the average AOD (0.55 μm) of the 7 sand and dust processes in April 2006 with the TOMS AI in the same period showed the simulated dust AOD was well consistent with the TOMS AI in East Asia and its adjacent West Pacific area. Both the simulated AOD and the TOMS AI data indicated that the SDS3 was the strongest dust process of all in terms of intensity, transport distance and affecting area in April 2006. This dust event had an important impact on Southern Mongolia, Northern and Northeast Inner Mongolia, Central and Eastern China as well as part of Eastern Japan. From its averaged status of the dust event, the AOD in Eastern China, including Beijing was over 3, and in Southern and Western Japan it accounted for 1, with AOD being consistent with TOMS AI in the affected area and center strength of dust. It was obvious that the simulated dust AOD center of the SDS3 and DS4 was rather weak in the Taklimakan Desert of the Western China while TOMS AI indicated that a pretty strong high-value centre existed in this region. The surface weather observation (Figure 4) showed that there was a long-period floating dust, instead of an up-blowing dust or dust storm during the two dust events in this area. This source area was far away from the Chinese inland and it is unlikely affected by other types of aerosols except for dust. All these suggest that the dust aerosol in this region was at higher altitude, which was not locally up-taken but probably from the Central Asian deserts beyond China. Since the domain of GRAPES-CUACE/Dust model does not cover deserts in Central Asia, which explains the failure to capture the floating dust weather in the Taklimakan Desert in Western China, hence this should not be attributed to the sand up-blowing mechanism of the model itself. The SDS2 simulation result further demonstrated the effectiveness of the model's sand up-blowing scheme for the Taklimakan area. The dust AOD center simulated by the model was consistent with the TOMS AI high-value area, revealing that the Taklimakan Desert had the strongest sand and dust aerosol extinction effect. Surface observations (Figure 4) also showed that several meteorological stations in the area had been observed firstly sand/dust storm and strong sand/dust storm dcvring 9—10 April. The analysis of average vertical sand/dust up-blowing flux in the model simulations also showed the Taklimakan Desert was the most important source of this severe sand/dust storms, further indicating that the model's sand/dust up-blowing scheme is applicable to this area. In terms of dust emission amount and intensity, SDS2 was equivalent to SDS3. However, compared with SDS3, the impact of SDS2 on the down-stream region was apparently weaker, and the transport distance was also shorter. This was mainly due to the fact that the Taklimakan Desert was located in the basin surrounded by mountains at an altitude over 3000 m, preventing it moving to the down-stream areas. DS 2 was similar to SDS 2 which was obviously stronger than DS 2 in terms of intensity. Both the optical depth given by the model and the TOMS AI show the Taklimakan Desert is the main source of the sand/dust storm. This further demonstrates that the model is still able to capture weaker sand/dust storm processes over the Taklimakan area. The simulation results of SDS1, DS1, DS3, DS4 (Figure 3) showed that the average AOD and TOMS AI had a very good consistency in the 4 processes. This also suggests that for both strong and relatively weak sand/dust events GRAPES-CUACE/Dust model agrees to actual observations well, indicating that the model outputs are acceptable.

It is well known that TOMS AI has its limitation in detecting aerosol at the surface layer. People are more concerned about the model capability to forecast surface dust storms and the accuracy and time validity of its forecast. The authors made a detailed comparison between the model-predicted 72-hour surface dust concentrations and surface weather observations of the 7 sand/dust storm processes in April 2006. In order to demonstrate in more details the model's capability to capture the processes of storm start, development, transport and weakening until disap pearance, the paper mainly selects SDS3, the strongest sand/dust storm in April 2006, for analysis (Figure 4). It could be seen from Figure 4 that the strong sand/dust storm broke out at 03:00 UTC in the morning of 16 April in Southern Mongolia,

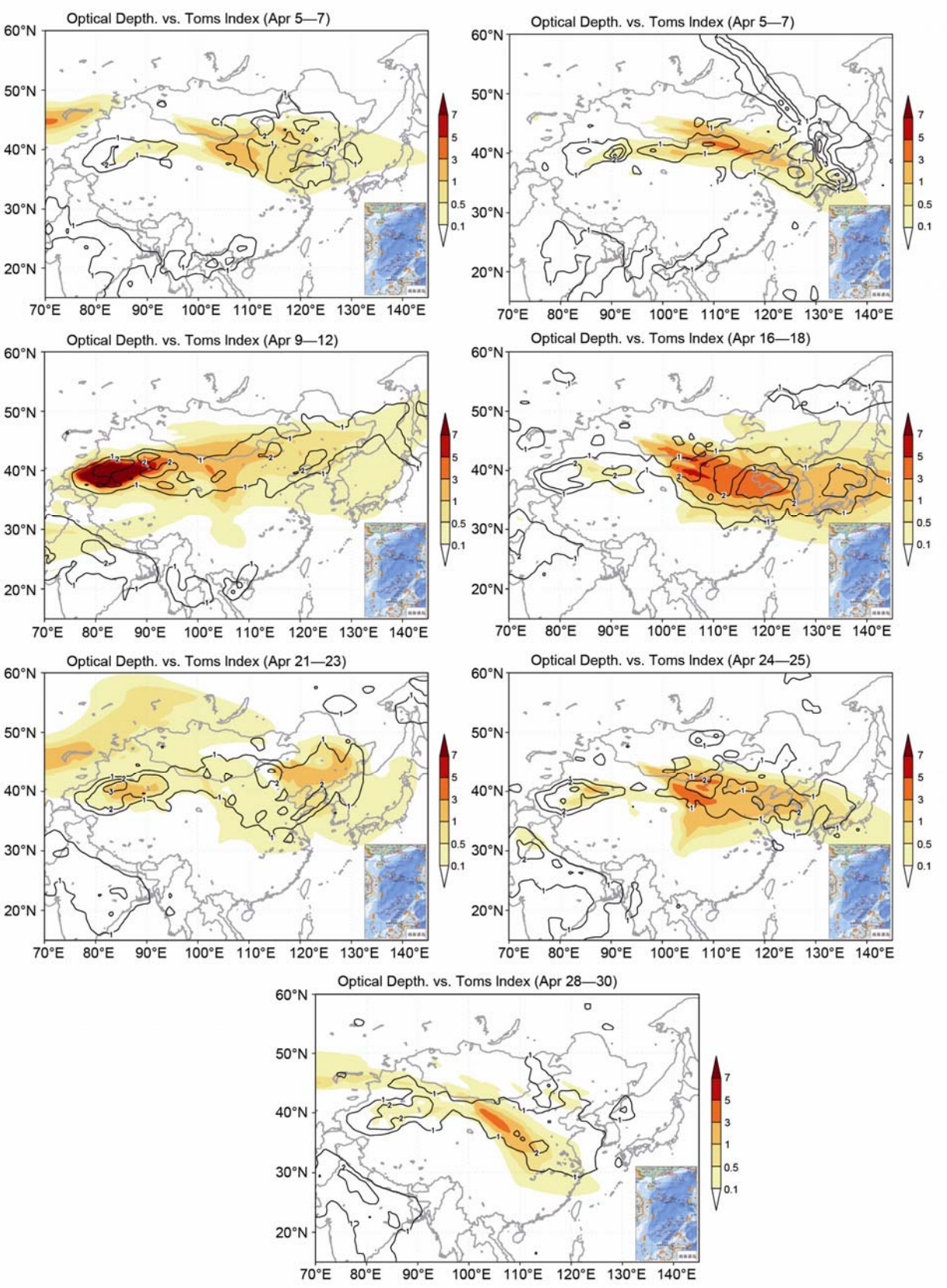

Figure 3 The dust AOD (0.55 μm) of the 7 sand and dust storms in April 2006 outputted by model and corresponding TOMS AI. The shaded area is the dust AOD, the contour is TOMS AI.

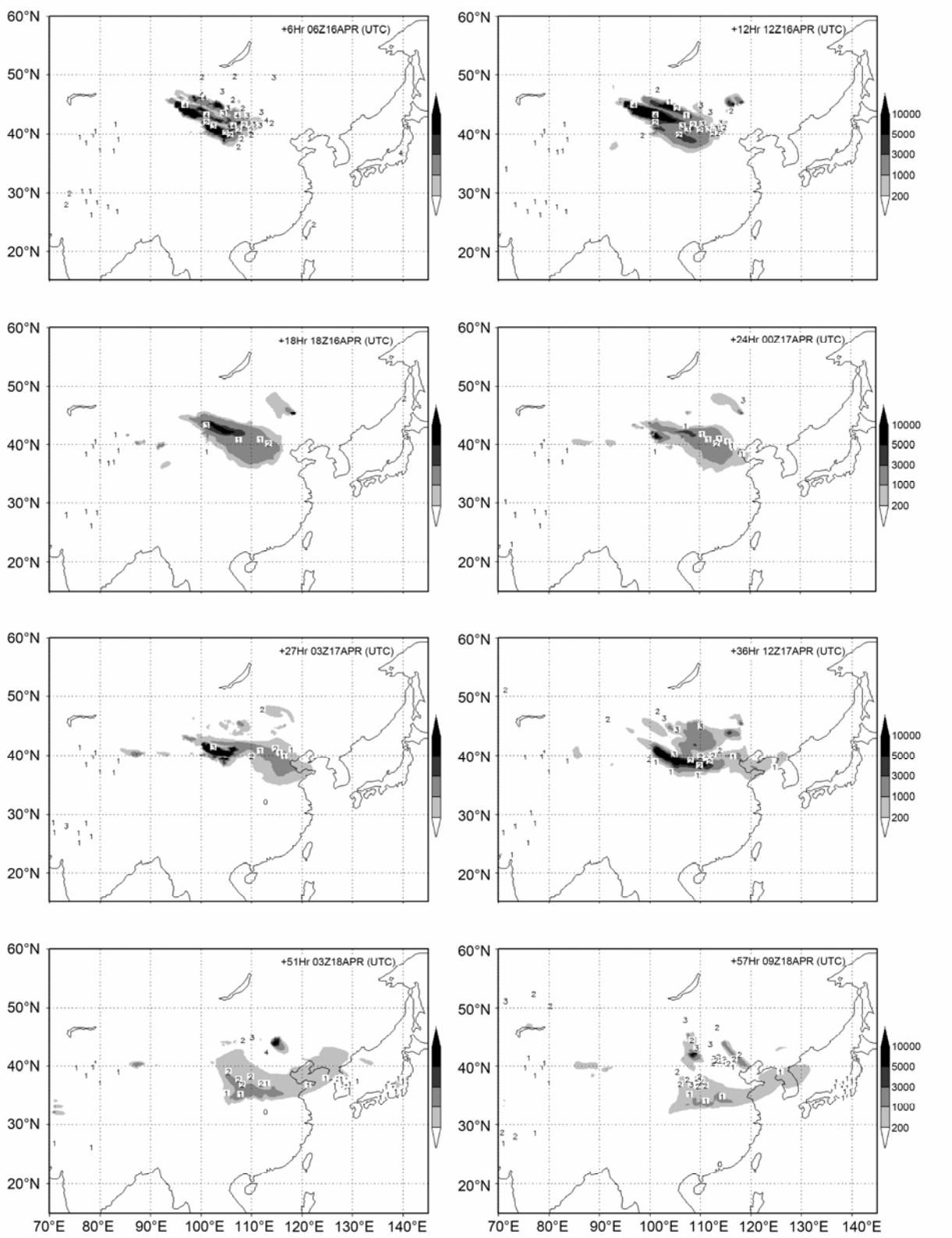

Figure 4 Surface dust concentration (shaded) from the model and surface weather observations (figures). 1, Floating dust; 2, blowing sand; 3, dust storm; 4, severe dust storm.

Sino-Mongolian border, Central and Northern Inner Mongolia deserts ranging from 95°E to 110°E. The model gave an accurate prediction in both the onset time and location. From 03:00 to 12:00 UTC, the sand/dust storm got strengthened and gradually moved to its down-stream region. The surface weather observations in several meteorological stations in this region at 09:00 UTC observed DS and SDS. The surface sand/dust concentration from the model also reached its maximum at this time. Moreover, the predicted domains with a concentration above 5000 μg/m^3 were in line with those areas where strong sand/dust storm was observed. After 12:00 UTC, due to the diurnal change of surface wind fields, the surface observations showed that the sand/dust storm was weakened significantly with a reduced coverage. The surface sand/dust concentration in the model from 18:00 UTC, 16 April to 00:00 UTC next day was decreased substantially relative to the daytime of the 16th, and its coverage shrank. This showed that the sand/dust up-blowing and deposition process described by the model could dynamically describe the diurnal change of the sand/dust weather. In the night of 16 April, the storm continued to move southeastwards while weakening. At 00:00 UTC, 17 April, both the model's forecasts and the observations revealed that the sand/dust storm was transported to the Eastern China, bringing floating dust and blowing sand to parts of central and eastern China. In the daytime, observations showed that the dusty weather got strengthened, and parts of central China met dust storm or floating sand/dust consequently. The simulation also showed that the surface sand/dust concentration in these areas picked up again in the daytime on 17 April, while both the observations and model outputs indicated that the sand/dust had been transported to the eastern coast of China and western Korean Peninsula. From the night of the 17 to 18 April, the sand/dust weather moved further eastwards. From 03:00 to 06:00 UTC on 18 April, both the Korean Peninsula and Japan witnessed floating dust at and the model gave a similar outcome of surface concentration of 200 μg/m^3. The analysis suggested that the model well captured the whole process of the sand/dust storm's onset, development, transport to its down-stream areas, while being weakened and gradual disappeared from 16 to 18 April 2006. The time validity, transport trajectory and diurnal variation of the sand/dust weather predictions were consistent with the observations. Similarly, for the other sand/dust events, the authors also treated them in the same way, with similar results as SDS3. The surface sand/dust event predictions in 72-hour by GRAPES-CUACE/Dust model had good consistency with the observations and the model showed good model performances.

Meanwhile, it should also be noted that the model has following weaknesses in comparison with TOMS AI or the surface observations. Firstly, the model missed some floating dust weather processes in Western China. Such missing was occasionally found in other regions often at the initial stages of the model (figures omitted) with a phenomena that the optical depth value over that region is apparently smaller than it should be, compared with TOMS AI and surface observations. Since the model's initial dust field of sand/dust concentration is set zero at present, the model will fail to capture any floating dust weather at its initial run, at which some areas has already met or are meeting floating dust weather. Practically, an improvement and address to this problem lies on the setup of appropriate initial field of the sand/dust concentration. A reasonable solution is to use the dust assimilated concentration data derived from satellite data instead for the dust zero initial filed. Concerning this work, the authors will give a detailed discussion and verification in a next paper. Secondly, to improve the accuracy of the model's quantitative predictions, more investigations are required in the following two aspects, i.e. quantitative comparisons of surface concentrations with PM10 values on the one hand, and with radar data on the other for more realistic vertical dust distribution profiles.

2.3 Sources of sand/dust emission

In accordance with the geological location and the impacts on downstream regions, the major sand/dust emission sources can fall into 3 components, i.e. Source 1: the deserts in the southern Mongolia, China-Mongolian border and central Inner Mongolia; Source 2: Taklimakan Desert in Xinjiang, and Source 3: Hunshandake sandy lands in NE Inner Mongolia (see Figure 5). All of these regions vary largely from their surrounding areas in topography. China-Mongolian border is 1000–2000 m above the sea level, but its adjacent area is vast grasslands and the Gobi desert. This region is a place where most Mongolian cyclones generate and pass through. It is the most important sand/dust source for the East Asia. The Taklimakan Desert is much larger than that along China-Mongolian border. The desert is situated in Xinjiang basin and its sea level is lower than its surrounding mountains, which are 3000–5000 m above the sea level with only a narrow NE passage leading to the downstream regions. Hunshandake sandy lands are the smallest region among these 3 sources, but it is the closest one with the downstream region. Though it is 1000 m high above sea level, it is prone to sand/dust emissions and causing considerable impacts on the downstream regions, as there is the significant difference in height and it is a junction of both northwesterly and northerly cold air.

The average vertical sand/dust emission fluxes in the 7 processes in April 2006 are calculated in this paper (Figure 6). The figure shows among the 7 sand/dust events, 5 processes (SDS1, SDS3, DS1, DS3 and DS4) were originated from Source 1, showing that the deserts along China-Mongolian border and in the Inner Mongolia was the major source for the East Asia. In addition, both average aerosol index (AI) and optical depth (Figure 1) also reflected that these processes brought about most high impacts on down

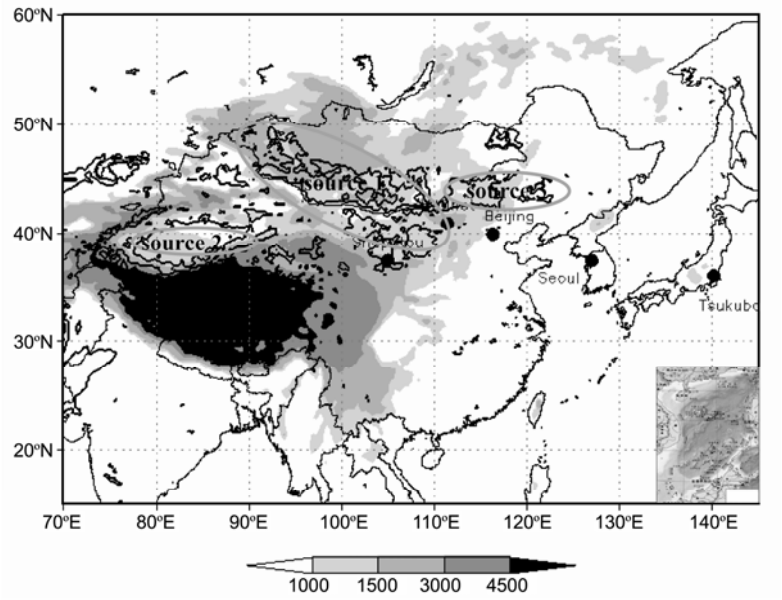

Figure 5 The main dust sources and topography height (in shadow).

stream regions, showing that Source 1 had the most severe impact on the downstream regions. Figure 6 shows that the SDS2 were due to both Sources 1 and 2. From the prospective of the sand/dust flux, Source 2 was a greater contributor compared with Source 1. Source 3 also partially contributed to SDS2.

The intensity of SDS2 was comparable to that of SDS1, but its primary source was located in the Taklimakan Desert and the mountains nearby prevent sand/dust from being transported to the downstream regions. Therefore, the observed strong sand/dust processes and high values in terms of TOMS AI and aerosol optical depth from the model were collocated in the Taklimakan Desert (Figure 4). In comparison with SDS1, SDS2 had less impact on the downstream. It is worth noting that though the Source 3 is not large in size, it contributed to SDS1, SDS2, SDS3, DS2 and DS4 with a greater intensity in sand/dust emissions. As being close to the downstream (eastern China), therefore the role of Source 3 cannot be ignored. To sum up, 2 out of 3 strong sand/dust processes were from Source 1, and 1 SDS was the combination of both Sources 1 and 2, based on the analysis of sand/dust emission fluxes given by the model. Moreover, though the Source 3 was not large, it contributed to all 3 strong sand/dust storms.

To further assess the sand/dust emissions over the East Asia in April 2006 and the respective contributions of 3 sources to the sand/dust storms, the paper presents the sand/dust emissions of the 7 dust storm processes in that month and their respective percentage to the total sand/dust emissions. The results suggested that the total emission from the major deserts was 225 million tons in East Asia April 2006 alone. Given the spring is high season for sand/dust storms and April experiences most severe and frequent sandy/dusty weather, such estimate is consistent with findings [27], which estimates the annual emission is 800 million tons over the same region. Out of 225 million tons, the deserts and sand lands in the northern Inner Mongolia and around China-Mongolian border contribute the most, namely 153 million tons, accounting for 68% of the total emissions. The Taklimakan Desert ranks second, contributing approximately 38 million tons or 17% of the total, and the Hunshandake sandy lands contributed the least, emitting about 15 million tons or accounting for 7% of the total emissions. The contributions from other deserts and abandoned farmlands were about 8% of the total.

From the above, in terms of occurrence frequency and emission volume, the deserts in northern China and China-Mongolian border are the most important sand/ dust sources, which exactly sit on the path of the Mongolian cyclones–the trigger of sand/dust process, and tracks of northwesterly and northerly cold air. In addition, the significant topographic difference between this region and its downstream areas facilitates the southeastward transport of sand/dust particles by the cold air, becoming the predominant source for sandy/dusty weather in central and eastern China and further beyond. The Taklimakan Desert is the second largest one in the world and the biggest in China. However, its emission only accounts for 17% of the total in April 2006. The reasons behind include its terrain constraint, lower frequency and weaker intensity of cold air outbreaks as well as low surface wind velocity. In particular, the terrain of the desert and the area nearby largely restrict the sand/dust transport to downstream, confining the impacts to the Xinjiang Basin and its adjacent area. Only when the weather system blows up the sand/dust into the air above 3000 meters, can these particles traverse the mountains

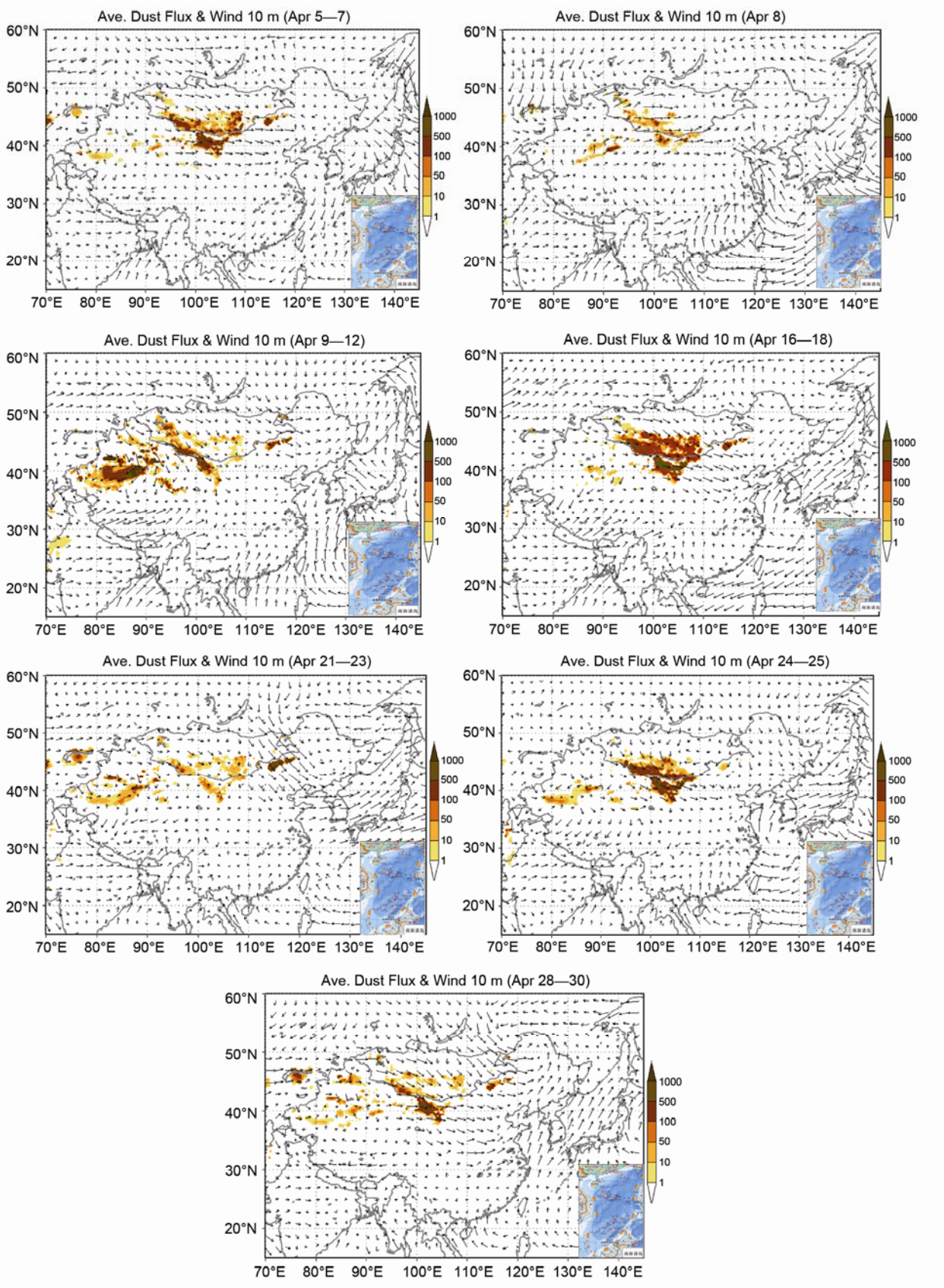

Figure 6 Average dust emission fluxes in 7 major sand/dust events in April 2006 (μg/m^2 s).

standing in the east and west and make the way to the downstream regions. Due to its small area, the Hunshan dake sandy lands emit the least in the 3 sources, only accounting for 7% of the total. But the frequency and intensity of emissions are high. As it is situated at the junction of both northward and northeast cold air and it is close to downstream outlet with a large topographic difference with downstream, attention should be given to the impact of this region upon the downstream regions, especially upon eastern China (Figure 7).

2.4 Dry and wet deposition

Sand/dust deposition refers to the amount of sand/dust particles falling down to the ground from atmosphere during a period of time over certain region. It directly shows the impact of sand/dust weather upon the lower atmosphere near the surface and the transportation distance of sand/dust particles and therefore is an important physical variable of dust events. However, few observations and modeling results describe the overall sand/dust deposition amount and its temporal and spatial distribution over East Asia due to some technical constraints. The aerosol deposition process consists of dry deposition, cloud removal and precipitation wash (wet deposition). The detailed calculation schemes of dust deposition processes are introduced in other studies [25,35]. However, the dry, wet and total deposition amounts, of the 7 major sand/dust events in April 2006 are given here and also their spatial distribution characteristics are analyzed. This study is promised to outline the deposition pattern for sand/dust events of April, the month in which sand/dust storms occurs most frequently over East Asia.

The calculated results showed that the a total of sand/dust deposition was about 136 million tons over the East Asia (70°–140°E, 15°–60°N) in April 2006, in which the dry deposition was 127 million tons which was approximately 94% of the total depositions, and the wet deposition was only 8 million tons, accounting for only 6% of the total. It was obvious that the distribution of dry deposition could represent a general distribution pattern of the total depositions. The spatial distribution of dry deposition (Figure 8(a)) showed that the most sand/dust particles deposited in the 3 dust source areas of China and east Asia and the palpable deposition process was also found in eastern China and

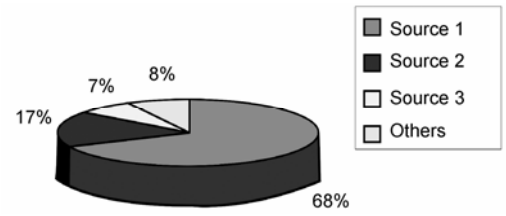

Figure 7 The percentage of sand/dust emissions of the 3 sources relative to the total emission.

off-shore region while the deposition amount was much less in the area east of the China Sea. The calculated deposition amounts in different areas (Figure 9) suggested that the total deposition amount in the 3 source regions was about 135 million tons, accounting for 78% of the total. Secondly, the deposition amount exceeded 2 million tons over the mainland China to the west of 120°E, accounting for 16% of the total. Only about 850 000 tons settled in the off-shore areas of the eastern China, Korea Japan, and the western Pacific between 120°–140°E, which was 6% of the total within the model domain. From the above it can be noted that in April 2006, about 94% dust particles deposited on the mainland to the west of 120°E, indicating that the East Asian sand/dust event has relatively minor impacts on the down-stream region and the Pacific east of 120°E.

In April, the most northern China dwell in spring-drought season, characterized with of less cloud and rainfall, particularly in most deserts and their adjacent areas, where the monthly rainfall is normally less than 1 mm. Compared with the dry deposition, the wet deposition is very small, accounting for only 6% of the total depositions. The wet deposition indicated a completely different distribution pattern from the dry deposition (Figure 8(b)), showing 2 wet deposition centers, one is located in the area extending from northeastern China to the Korean Peninsula and the ocean west of Japan. This was mainly due to the fact that the air humidity in this area was higher than in the source areas, with relatively more clouds compared with its surrounding areas. Furthermore, there was light rainfall during April 16–18 in this area, which led to wet deposition. Another wet deposition center was found in the areas around the Xinjiang basin. The formation of this center may be possibly due to the presence of orographic clouds in the Tarim Basin, which caused the wet deposition. A more detailed discussion on further analysis of wet deposition and its attributions will be addressed in the follow-up papers.

3 Conclusions and discussion

Based on regional forecasting model GRAPES-Meso of China new-generation Global/Regional Assimilation and PrEdiction System(GRAPES) and the Atmospheric Chemistry Module (CUACE) developed by CAWAS, a mesoscale sand/dust forecasting system GRAPES-CUACE/Dust model has been established. It adopts a semi-implicit & semi-Lagrangian transport scheme with good positive definite conservation. Model tests show good performance in mass conservation in the model integral process. The physical process schemes is optimized and selected in the context of the weather and climate characteristics over East Asia in this paper. The model contains a detailed aerosol process. The incorporation of the latest land desertification data over China and snow cover derived from real-time satellite data

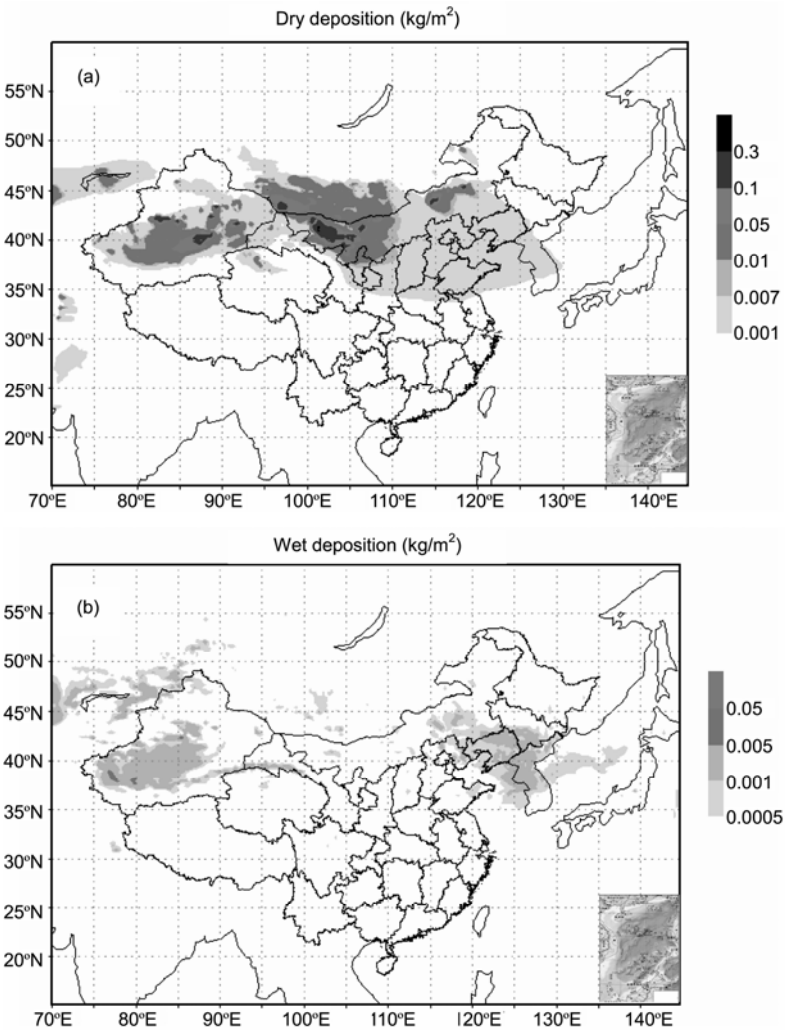

Figure 8 The distribution of dry (a) and wet (b) depositions in April 2006

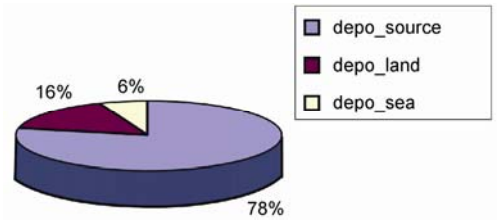

Figure 9 Deposition proportions (percentage) in different areas.

make the sand/dust up-blowing process more reasonable. The comparison of model outputs of major sand/dust weather events in April 2006, with surface observations and aerosol indices derived from ozone spectrophotometers (TOMS AI) shows that overall model performance is reasonable, which gives an objective description of the occurrence, evolution, transportation to the down streams, weakening till disappearance of the dust weather events. The time validity, transport pathways and the diurnal variations of model outputs are highly consistent with the observations.

Based on GRAPES-CUACE/Dust model, the analysis of major sand/dust events in April 2006 including the up-blowing sand/dust and deposition processes shows that the 7 major events took place in April 2006 and totally about 225 million tons of sands/dusts were emitted into the atmosphere. The major source regions were the deserts around the China-Mongolia border with a contribution of 153 million tons that accounted for 68% of the total emissions, Taklimakan Desert ranking second and contributing approximately 38 million tons or 17% of the total, and the Hunshandake sandy lands that emitted about 15 million tons or 7% of the total. The 3 major sources were also the major deposition areas. The depositions in the 3 major sources accounted for 78% of the total. The secondary deposition area was the mainland China accounting for 16% of the total deposition. The deposition over the region east of 120°E including China's off-shores, Korean Peninsula, Japan and the North Pacific took only 6% of the total. Dry deposition dominated, accounting for 94% of the total dust depositions in April 2006 since it was generally dry with

less rainfall over northern China in April. And wet deposition was relatively less only 6%, which concentrated in Xinjiang basin, the area from northeastern China to the Korean Peninsula and the sea west of Japan.

Meanwhile, GRAPES-CUACE/Dust model has the following deficiencies and should be improved: The floating dust weather events over the western China and other individual areas were missed at the model beginning. The reason is the model uses the zero dust initial fields and the sand/dust sources abroad, west of Xinjiang, are not included in the model domain. It was unavoidable to miss the floating dust weather events which had already existed at the initial run of the model or those dust transported from the upper stream source regions beyond the model domain. The key solution to the problem is to use the assimilated sand/dust data of observed into the model initial field to replace the zero initial concentration fields at the initial model run. At present, the real-time satellite data assimilation and model application are under way and related schemes and outcomes will be dealt with in a separate paper. Besides, there are deficiencies in verification of model outputs with quantitative observations, especially an urgent need to compare the surface dust/sand concentrations from the model with PM 10 and their vertical distribution with LIDAR data, so as to further optimize and improve the model's predictability in capturing surface dust/sand concentrations and their vertical distribution. Such efforts can not only improve the accuracy of the model predictions, but can be beneficial to more accurately calculating dust/sand radiation effects the feedback mechanism of short-term weather regimes on the radiation effects.

This work was supported by the National Basic Research Program of China (*Grant No. 2006CB403705*)*, National Special Public Sector Research* (*Grant No. GYHY*(*QX*)*2007-6-36*) *and National Science and Technology Project of China* (*Grant No. 2008BAC40B02*).

1 Zhuang G S, Guo J H, Yuan H, et al. The composition, source, particle size distribution of dust storms in China in 2000 and its effects on the global environment. Chinese Sci Bull, 2001, 46: 191–197
2 Han Y X , Song L C, Zhao T L, et al. The relationship between continental dust and marine phytoplankton in the North Pacific and its impact on marine phytoplankton. Chin Environl Sci, 2006, 26: 157–160
3 Wang Z, Akimoto H, Uno I. Neutralization of soil aerosol and its impact on the distribution of acid rain over East Asia: observations and model results. J Geophy Res, 2002, 107: 4389, doi: 10.1029/2001JD001040
4 Carlson T N, Benjamin S. Radiative heating rates for Sahara dust. J Atmos Sci, 1980, 37: 193–197
5 Wang H, Shi G Y, Wang B, et al. Chinese desert dust aerosols and atmosphere radiation heating characteristics in North Pacific Region. Chin J Atmos, 2007, 31: 515–526
6 Wang H, Shi G Y, Teruo A, et al. Radiative forcing due to dust aerosol over east Asia-north Pacific region during spring 2001. Chinese Sci Bull, 2004, 49: 2212–2219
7 Claquin T. Uncertainties is assessing the radiative forcing by mineral dust. Tellus Ser B, 2000, 50: 491–505
8 Duce R A. Sources, distributions, and fluxes of mineral aerosols and their relationship to climate. In: Charlson R J, Heintzenberg J. Aerosol Forcing of Climate. New York: John Widely, 1995
9 Hansen J, Sato M, Ruedy R, et al. Forcing and chaos in interannual to deca dal climate change. J Geophys Res, 1997, 102: 25679–25720
10 Sokolik I N, Winber D M, Bergametti G, et al. Introduction to special section: Outstanding problems in quantifying the radiative impacts of mineral dust. J Geophys Res, 2001, 106: 18015–18027
11 Tegen I, Lacis A A, Fung I. The influence on climate forcing of mineral aerosols from disturbed soils. Nature, 1996, 380: 419–422
12 Tegen I, Fung I. Modeling of mineral dust in the atmosphere: Sources transport and optical thickness. J Geophys Res, 1994, 99: 22897–22914
13 Tegen I, Hollrig P, Chin M, et al. Contribution of different aerosol species to the global aerosol extinction optical thickness: Estimates from model results. J Geophys Res, 1997, 102: 23895–23916
14 Takemura T, Nakajima T. Single-scattering albedo and radiative forcing of various aerosol species with a global three-dimensional model. J Clim, 2002, 4: 333–352
15 Toon O B, Turco R P, Westphal D, et al. A multidimensional model for aerosols, description of computational analogs. J Atmos Sci, 1998, 45: 2123–243
16 Nickovic S, Dobricic S. A model for long-range transport of desert dust. Mon Weather Rev, 1996, 124: 2337–2345
17 Westphal D, Toon O B, Carlson T N. A two-dimensional numerical investigation of the dynamics and microphysics of Saharan dust storms. J Geophys Res, 1987, 92: 327–3049
18 Prospero J M. Long-range transport of mineral dust in the global atmosphere: Impact of African dust on the environment of the Southeastern United States. Proc Natl Acad Sci, 1999, 99: 3396–3403
19 Kalma J D, Speight J G, Wasson R J. Potential wind erosion in Australia, A continental perspective. J Atmos Sci, 1988, 8: 411–428
20 Husar R B. Asian dust events of April 1998. J Geophys Res, 2001, 106: 18317–18330
21 Wang Z, Ueda H, Huang M. A deflation module for use in modeling long-range transport of yellow sand over East Asia. J Geophy Res, 2000, 105: 26947–26960
22 Lasserrea F, Cauteneta G, Alfarob S C, et al. Development and validation of a simple mineral dust source inventory suitable for modelling in North Central China. Atmos Environ, 2005, 39: 3831–3841
23 Zhao L N, Sun J H, Zhao S X. Numerical simulation of dust emission in North China and Beijing. Clim Environ Res, 2002, 7: 279–294
24 Chen C L, Wang Y C, Liu W D, et al. Regional dust and sand profile model coupled with the dynamic field and cases simulation. Chinese Sci Bull, 2004, 49: 2007–2013
25 Gong S L, Zhang X Y, Zhao T L, et al. Characterization of soil dust aerosol in China and its transport and distribution during 2001 ACE-Asia: 2. Model simulation and validation. J Geophys Res, 2003, 108: 4262, doi: 10.1029/2002JD002633
26 Zhang X Y, Gong S L, Zhao T L, et al. Sources of Asian dust and role of climate change versus desertification Asian dust emission. J Geophys Res, 2003, 30: 2272, doi: 10.1029/2003GL018206
27 Zhang X Y. Source distribution, emission, transport, deposition of Asian dust and loess accumulation. Quat Sci, 2001, 21: 29–40
28 Yang X S, Chen J B, Hu J L, et al. A semi-implicit semi-Lagran global nonhydrostatic model and the polar discretization scheme. Sci China Ser D-Earth Sci, 2007, 50: 1885–1891
29 Zhuang S Y, Xue J S, Zhu G F, et al. GRAPES global 3D-Var System—Basic scheme design and single observation test. Chin J Atmos, 2005, 29: 872–884
30 Staniforth A, Cote J. Semi-Lagrangian integration scheme for atmospheric models—A review. Mon Weather Rev, 1991, 119: 2206–2223
31 Arakawa A, Lamb V R. Computational Design of the Basic Dynamical Processes of the UCLA General Circulation Model. Methods in Computational Physics, General Circulation Models of the Atmosphere. New York: Academic Press, 1997. 1–17
32 Charney J L, Philips N A. Numerical Integration of the quasi-geostrophic equations for barotropic and simple barotropic flow. Meteor, 1953, 10: 71–99
33 Hong S Y, Pan H L. Nonlocal boundary layer vertical diffusion in

a medium-range forecast model. Mon Weather Rev, 1996, 124: 2322–2339
34 Chen D H, Xue J S, Yang X S, et al. The new generation of hydrostatic/nonhydrostatic multi-scales numerical prediction model: Scientific design and experiments (in Chinese). CAMS Technical Report 1. 2003
35 Gong S L, Zhang X Y. CUACE/Dust—an integrated system of observation and modeling systems for operational dust forecasting in Asia. Atmos Chem Phys, 2008, 8: 2333–2340
36 Zhou C H, Gong S L, Zhang X Y, et al. Development and evaluation of an operational SDS forecasting system for East Asia: CUACE/Dust. Atmos Chem Phys, 2008, 8: 787–798
37 Dickinson R E, Henderson-Sellers A, Kennedy P J, et al. Biosphere-atmosphere transfer scheme (BATS) for the NCAR community climate model. NCAR Technical, 1986. 1–69
38 Yang Y Q, Hou Q, Zhou C H, et al. Sand/dust storm processes in Northeast Asia and associated large-scale circulations. Atmos Chem Phys, 2008, 8: 25–33
39 Zhang X Y, Gong S L. The Sand and Dust Storm of Northeast Asia in Spring 2006. Beijing: Meteorology Publishing Company, 2006. 1–118
40 Herman J R, Bhartia P K, Torres O, et al. Global distribution of UV-absorbing aerosols from Nimbus 7/TOMS data. J Geophys Res, 1997, 102: 16911–16922